Acta Biochim Biophys Sin 2023, 55(5): 749–757
https://doi.org/10.3724/abbs.2023083
Advance Access Publication Date: 15 May 2023
Original Article

Original Article

Activation of Kir2.1 improves myocardial fibrosis by inhibiting Ca^{2+} overload and the TGF-β1/Smad signaling pathway

Yi Rong[1,2,3,†], Xin Zhou[1,2,3,†], Zhenli Guo[1,2,3,†], Yingying Zhang[1,2], Wenjuan Qin[1,2], Li Li[1,2], Junqiang Si[1,2,3], Rui Yang[1,2,3,*], Xinzhi Li[1,2,4,*], and Ketao Ma[1,2,3,*]

[1]The Key Laboratory of Xinjiang Endemic and Ethnic Diseases, Ministry of Education, Shihezi University Medical College, Shihezi 832002, China, [2]NHC Key Laboratory of Prevention and Treatment of Central Asia High Incidence Diseases, Shihezi 832002, China, [3]Department of Physiology, Shihezi University Medical College, Shihezi 832002, China, and [4]Department of Pathophysiology, Shihezi University Medical College, Shihezi 832002, China

[†]These authors contributed equally to this work.

*Correspondence address. Tel: +86-15001645180; E-mail: maketao@hotmail.com (K.M.) / Tel: +86-13309939180; E-mail: lixinzhi@shzu.edu.cn (X.L.) / Tel: +86-18299092816; E-mail: 458360505@qq.com (R.Y.)

Received 31 August 2022 Accepted 8 December 2022

Abstract

The inwardly rectifying potassium channel Kir2.1 is closely associated with many cardiovascular diseases. However, the effect and mechanism of Kir2.1 in diabetic cardiomyopathy remain unclear. *In vivo*, we use STZ to establish the model, and ventricular structural changes, myocardial inflammatory infiltration, and myocardial fibrosis severity are detected by echocardiography, histological staining, immunohistochemistry, and western blot analysis, respectively. *In vitro*, a myocardial fibrosis model is established with high glucose. The Kir2.1 current amplitude, intracellular calcium concentration, fibrosis-related proteins, and TGF-β1/Smad pathway proteins are detected by whole-cell patch clamp, calcium probes, western blot analysis, and immunofluorescence, respectively. The *in vivo* results show that compared to diabetic cardiomyopathy, zacopride (a Kir2.1 selective agonist) significantly reduces the left ventricular systolic diameter and diastolic diameter, increases the left ventricular ejection fraction and left ventricular short-axis shortening, improves the degree of cell necrosis, and reduces the expression of myocardial interstitial fibrosis protein and collagen fibre deposition area. The *in vitro* results show that the current amplitude and protein expression of Kir2.1 are both decreased in the high glucose-induced myocardial fibrosis model. Additionally, zacopride significantly upregulates the expression of Kir2.1 and inhibits the expressions of the fibrosis-related proteins α-SMA, collagen I, and collagen III. Activation of Kir2.1 reduces the intracellular calcium concentration and inhibits the protein expressions of TGF-β1 and p-Smad 2/3. Activation of Kir2.1 can improve myocardial fibrosis induced by diabetic cardiomyopathy, and the possible mechanism may be related to inhibiting Ca^{2+} overload and the TGF-β1/Smad signaling pathway.

Key words diabetic cardiomyopathy, myocardial fibrosis, Kir2.1, Ca^{2+}, TGF-β1/Smad

Introduction

Diabetic cardiomyopathy (DCM) is the most common complication of diabetes and one of the main factors leading to heart failure, cardiogenic shock, and even death in diabetic patients [1,2]. Pathophysiological studies have found that myocardial fibrosis is an essential pathological mechanism of DCM. It is characterized by an imbalance of the extracellular matrix leading to excessive collagen deposition, which changes the cardiac structure, impairs the systolic and diastolic functions of the heart, and eventually leads to heart failure [3]. Furthermore, a previous study showed that persistent hyperglycemia can lead to hyperactivation of cardiac fibroblasts (CFs) and induce differentiation into myofibroblasts, leading to a cardiac extracellular matrix imbalance and myocardial fibrosis [4]. At present, the number of patients with DCM is still increasing worldwide, making the prevention and treatment of diabetic cardiomyopathy are of critical significance for diabetic patients.

Various ion channels are expressed on human and rat cardiac fibroblasts [5,6]. The inwardly rectifying potassium channel (IK1) determines the resting membrane potential of fibroblasts. Kir2.1 is the major subunit of the cardiac fibroblast IK1 channel. van Vliet *et al.* [7] reported that overexpression of Kir2.1 could cause membrane potential hyperpolarization, resulting in the increased expressions of cardiac-specific genes and proteins and the formation of spontaneously beating cardiomyocytes in human cardiac progenitor cells. Another study found that in a model of myocardial fibrosis and ventricular remodelling induced by angiotensin II, selective activation of the IK1 channel may have an anti-ventricular remodelling effect by reducing the activity of fibroblasts and inducing their apoptosis [8]. However, whether Kir2.1 is involved in the regulation of fibrosis in diabetic cardiomyopathy rats has not been reported.

Zacopride (Zac) is a selective agonist of Kir2.1 that can significantly improve myocardial interstitial remodelling after myocardial infarction in rats [9]. Moreover, Zac can inhibit cell death by reducing calcium overload or oxidative stress in ventricular myocytes [8]. Intracellular Ca^{2+} is closely related to the activation of multiple signaling pathways associated with fibrosis. Yuan *et al.* [3] reported that in the DCM model, the expressions of calcium-sensing receptors (CaSR) in myocardial fibroblast cell membranes were increased the intracellular Ca^{2+} concentration and further activated the TGF-β1/Smad signaling pathway, which promoted the proliferation and activation of fibroblasts and accelerated the onset and development of myocardial fibrosis.

In the present study, we aimed to establish a diabetic cardiomyopathy model to investigate whether pretreatment with the Kir2.1 agonist Zac could ameliorate ventricular myocyte fibrosis in diabetic cardiomyopathy rats by regulating the Ca^{2+} and TGF-β1/Smad signaling pathways.

Materials and Methods

Experimental animals

Sixty male SD rats (6 weeks) were provided by the Xi'an Animal Research Center [SCXK 2019 (Lu) 0003; Xi'an, China]. Suckling mice (1–3 days) were provided by the Animal Experimental Feeding Center of Shihezi University (Shihezi, China). All rats were kept under standard conditions, suitable temperature, moderate humidity and light, regular feed replacement, bedding, and purified drinking water. Sixty SD rats were free to eat food and drink water for 2 consecutive weeks. The rats were randomly divided into the control, DCM, DCM + Zac, and Zac groups. Four groups of rats were fed with a standard diet; the DCM and DCM + Zac groups were induced by streptozotocin (STZ, streptozocin, 60 mg/kg, single injection; Sigma, St Louis, USA) to yield a diabetic cardiomyopathy model. The control group was injected with the same dose of sodium citrate buffer. After 3 days, the random blood glucose of the rats in each group was measured. A random blood glucose measurement ≥16.7 mM indicated that the diabetic model was successfully established. The DCM + Zac group was given Zac (15 μg/kg·d; APExBIO, Houston, USA) for 10 weeks after the random blood glucose was ≥ 16.7 mM for 14 consecutive days. At week 12, the hearts of all the rats were harvested for subsequent experiments.

Cell culture

Cardiac fibroblasts were isolated from the hearts of 1- to 3-day-old suckling mice under sterile conditions. The isolated ventricular fibroblasts were cultured in Dulbecco's modified Eagle's medium (DMEM; Gibco, Carlsbad, USA) containing 10% fetal bovine serum (FBS; Gibco) and precooled in advance. After 2 h, the supernatant was discarded and washed three times with phosphate-buffered saline (PBS). Next, 10% complete medium was added to continue the culture. After 12 h, the medium was changed, and after 24 h, ventricular fibroblasts were measured at a density of > 90%. The P_1–P_3 ventricular fibroblasts were identified by immunofluorescence microscopy.

Echocardiogram test

Echocardiogram was recorded using the PHILIPS EPIQ7C cardiovascular ultrasound diagnostic apparatus (Amsterdam, Netherlands) equipped with an S12-4 matrix probe and a probe frequency of 4–12 MHz. The online analysis software QLAB12.0 was used to place the left lateral position of the anaesthetized rats on the examination table. The limbs and incisors of the rats were fixed with a rubber band, and the electrocardiogram of small animals was connected. The probe was placed at the left edge of the sternum, and the long axis section near the sternum was displayed. The routine cardiac values of rats in each group were measured: left ventricular internal diastolic dimension (LVIDd), left ventricular internal dimension in systole (LVIDs), left ventricular fractional shortening (LVFS), and left ventricular ejection fraction (LVEF). The two-dimensional images of the M-mode ultrasound curve clearly showed the rats' left ventricular wall and chamber conditions.

Histopathological examination

The heart specimens of the rats in each group were fixed in 10% phosphoric acid-buffered formalin and subjected to routine histological treatment. After paraffin embedding, the slices were dewaxed, and the heart was cut into 5-μm sections using a low-temperature thermostat. After hematoxylin-eosin staining (HE), the cross-sectional area of muscle fibres was measured using a microscope (Olympus, Tokyo, Japan) under a high-power field of view (HPF; 400 × , magnification). The degree of interstitial fibrosis in each group was detected by Masson's trichrome and Sirius scarlet staining. The interstitial collagen content was evaluated by analyzing the images of each group. The total collagen area was calculated and expressed as a percent of the total ventricular area.

Immunohistochemistry

The heart tissue of rats was washed with cold PBS and fixed with 10% phosphate-buffered formalin for 24 h. The myocardial fibrosis markers were detected by staining the rat heart tissue sections with antibodies against α-SMA (1:100; Boster, Beijing, China), collagen I (1:100; Boster), collagen III (1:100; Boster), and Kir2.1 (1:100; Abcam, Cambridge, UK). Six fields of view were randomly selected for microscopic observation from each specimen under a light microscope at 400 × magnification. The brown sections were observed. The myocardial fibrosis markers and the percentage of Kir2.1 (brown sections) in the entire myocardial area were calculated by Image-Pro plus 6.0 image analysis software (Media Cybernetics, Silver Spring, USA). In addition, GraphPad Prism 8 software (GraphPad, La Jolla, USA) was used to count the positive immunohistochemical staining (brown staining).

Western blot analysis

The protein samples (10 μL) were separated by 10% SDS

polyacrylamide gel electrophoresis, and transferred to a PVDF membrane (Millipore, Billerica, USA). Next, the membranes were blocked with 5% skim milk or 5% bovine serum albumin at 25°C for 2 h and then incubated with primary antibodies in the refrigerator overnight in a shaker at 4°C. The following antibodies were used: Kir2.1 (1:1000; Abcam), α-SMA (1:1000; Boster), collagen I (1:1000; Boster), collagen III (1:1000; Boster), TGF-β1 (1:1000; Abcam), Smad 2 (1:1000; Boster), p-Smad 2 (1:1000; Boster), Smad 3 (1:1000; Boster), p-Smad 3 (1:1000; Boster), and GAPDH (1:1000; Zhong Shan-Golden Bridge, Beijing, China). Next, the membranes were incubated with the corresponding HRP-conjugated secondary antibody at room temperature for 2 h, followed by three times wash with TBST for 10 min each. Finally, the ECL luminescence reagent (Biosharp, Hefei, China) was used to visualize the protein bands, and band density was analyzed on a Tanon-5200 gel imaging system (Tanon, Shanghai, China).

Immunofluorescence microscopy

After culturing and incubation for 24 h, the cells were washed with PBS three times (2 min each) and then fixed with paraformaldehyde for 10 min. After being washed with PBS three times (2 min each), the cell membrane was permeabilized with Triton X-100 for 1–3 min and then washed again with PBS three times (2 min each). After blocking with 10% BSA for 30 min, the antibodies were incubated with anti-Kir2.1 (1:100; Abcam), anti-α-SMA (1:100; Boster), anti-collagen I (1:100; Boster), or anti-collagen III (1:100; Boster) antibodies at 4°C overnight. After 30 min of rewarming the next day, the corresponding fluorescein-labelled antibody was added and incubated for 2 h at 37°C. PBS was used to wash the cells three times (10 min each). DAPI was used to stain the nuclei for 10 min, and then cells were observed under a fluorescence microscope (Solarbio, Beijing, China), and images were captured. ImageJ software (NIH, Bethesda, USA) was used for fluorescence image analysis.

Patch clamp

Cardiac fibroblasts were placed on an invert Nikon Diphot microscope (Tokyo, Japan) at room temperature (22°C). Microelectrodes with resistance values of 3–8 MΩ were selected to fill the electrode liquid (130 mM K-gluconate, 10 mM NaCl, 1 mM $MgCl_2$, 2 mM $CaCl_2$, 5 mM EGTA, 10 mM HEPES, and 5.5 mM glucose). Next, the glass microelectrodes filled with the intracellular fluid were connected to the micromanipulator. The electrode tip contacted the cells, and a slight increase in the electrode resistance was observed from the membrane test window. Mouth suction produced negative pressure in the microelectrode, and the clamping potential was gradually adjusted to –60 mV. After the cell is closely fitted to the electrode tip, and the resistance reaches GΩ, negative pressure was applied, and the auxiliary electrode was used to break the membrane. Under voltage-clamp mode, the cell membrane current was detected by the patch-clamp amplifier, and the membrane current was filtered at a low frequency of 5 or 10 kHz (–3 dB). The data were analyzed using pCLAMP software (Axon Instruments, San Diego, USA) and Photoshop software, and the isochronous current-voltage (I–V) curve was plotted.

Calcium probe

A 5-μM Fluo-3 AM (calcium ion probe; Abcam) working solution was prepared and stored at 37°C in the dark. Cells were washed three times with PBS and continued to culture for 40 min, and then washed again after adding the same volume of PBS and incubating for 30 min. The distribution of calcium ions in the ventricular fibroblasts was observed under a fluorescence microscope and the changes in intracellular calcium concentration were detected.

Statistical analysis

The statistical software GraphPad Prism 8 was used to analyze the results, which are expressed as the mean ± standard deviation (SD). One-way analysis of variance (ANOVA) and Student's *t*-tests were used to compare the differences. $P < 0.05$ was considered statistically significant.

Results

Activation of Kir2.1 ameliorates myocardial morphological changes induced by DCM

The DCM model was first prepared, and STZ was used for a single intraperitoneal injection. Figure 1A shows the simulation diagram of the *in vivo* experiment. The rats' blood glucose and body weight fluctuations were detected at 1, 3, 7, 14, 30, 60, and 90 days after modelling. After 90 days, myocardial structural changes of the rats in each group were detected by echocardiography. After successful modelling, cardiac histology staining and protein imprinting experiments were performed. As shown in Figure 1B, the body weight of DCM rats began to decrease after 60 days of modelling, and the same trend appeared after Zac treatment. By observing the heart morphology, we found that the hearts of the DCM rats were increased significantly, and the heart morphology was close to normal after Zac treatment (Figure 1C). After 7 days of modelling, the random blood glucose of the DCM rats was higher than 16.7 mM, and there was no significant change after Zac treatment (Figure 1D). The echocardiographic results showed that compared with those of the control group, the LVEF and LVFS of the experimental group were significantly decreased. Meanwhile, Zac administration alone had no significant effect on LVEF% and LVFS% in rats compared to the normal group (Figure 1E–J). In addition, HE, Masson's trichrome staining, and Sirius scarlet staining were used for histological observation. The myocardial fibres of the DCM rats were broken and partially disorganized, and there were many necrotic foci (Figure 2A). Furthermore, increased collagen deposition was observed (Figure 2B,C). After Zac treatment, the myocardial fibres were arranged neatly, the cell morphology was close to normal, and collagen deposition was significantly reduced (Figure 2B–E). Zac alone had no significant effect on cardiac structure.

Zacopride upregulates the expression of cardiac Kir2.1 protein and improves myocardial fibrosis in DCM rats

The expressions of myocardial fibrosis-related proteins were detected by western blot analysis and immunohistochemistry. The results showed that the protein expression of Kir2.1 was decreased in DCM ratscompared with the control group, and the protein expression of Kir2.1 was upregulated after administration of Zac. The effects of Zac on myocardial fibrosis in DCM were further explored by detecting the expression changes in the myocardial fibrosis markers α-SMA, collagen I, and collagen III. The results showed that compared with those in the normal group, the expressions of fibrotic proteins in DCM rats were increased, and Zac treatment ameliorated the degree of DCM-induced myocardial fibrosis (Figure 3A). The immunohistochemical results further

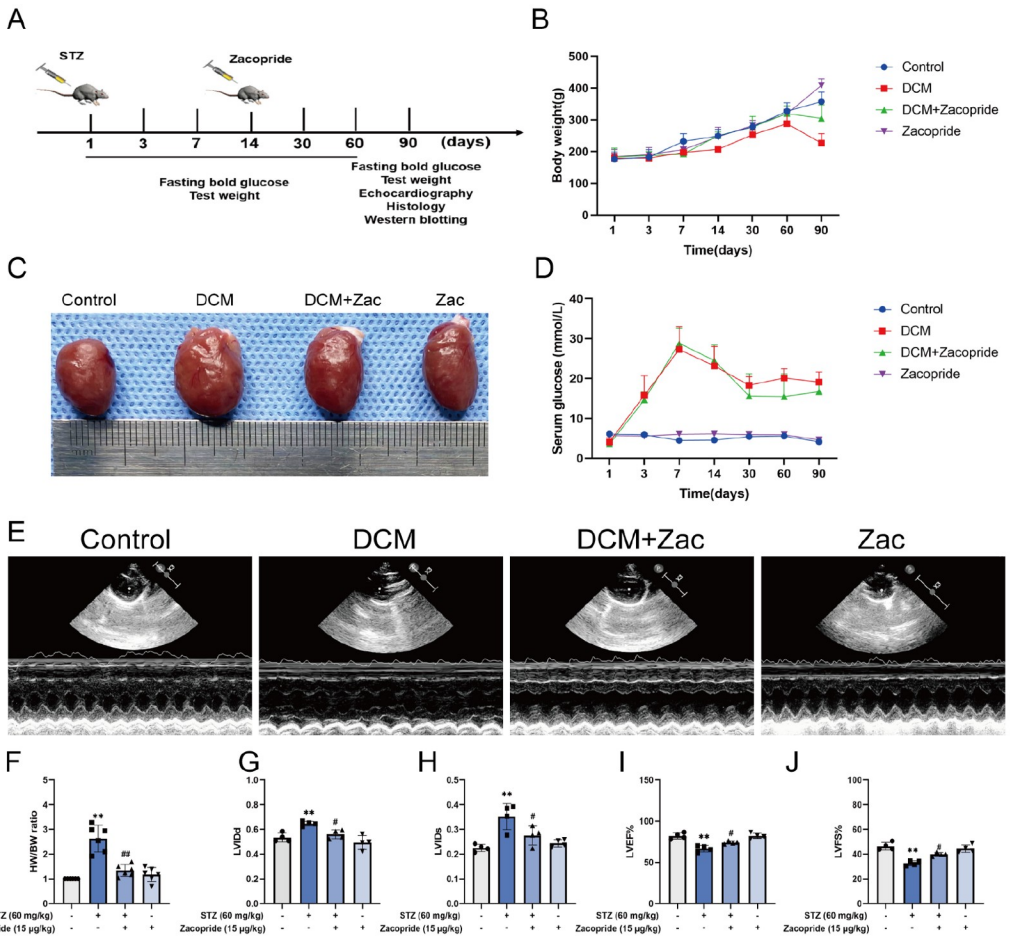

Figure 1. STZ-induced DCM model (A) Schematic diagram of *in vivo* experiment. (B) Weight fluctuations. (C) General morphology of the whole heart ($n = 6$). (D) Blood glucose fluctuations. (E) Cardiac ultrasound images ($n = 4$). (F) Ratio of heart weight to body weight. (G–J) The statistics of LVIDd, LVIDs, LVEF and LVFS in ultrasonic experiments. $^{**}P < 0.01$ vs control; $^{\#}P < 0.05$, $^{\#\#}P < 0.01$ vs DCM.

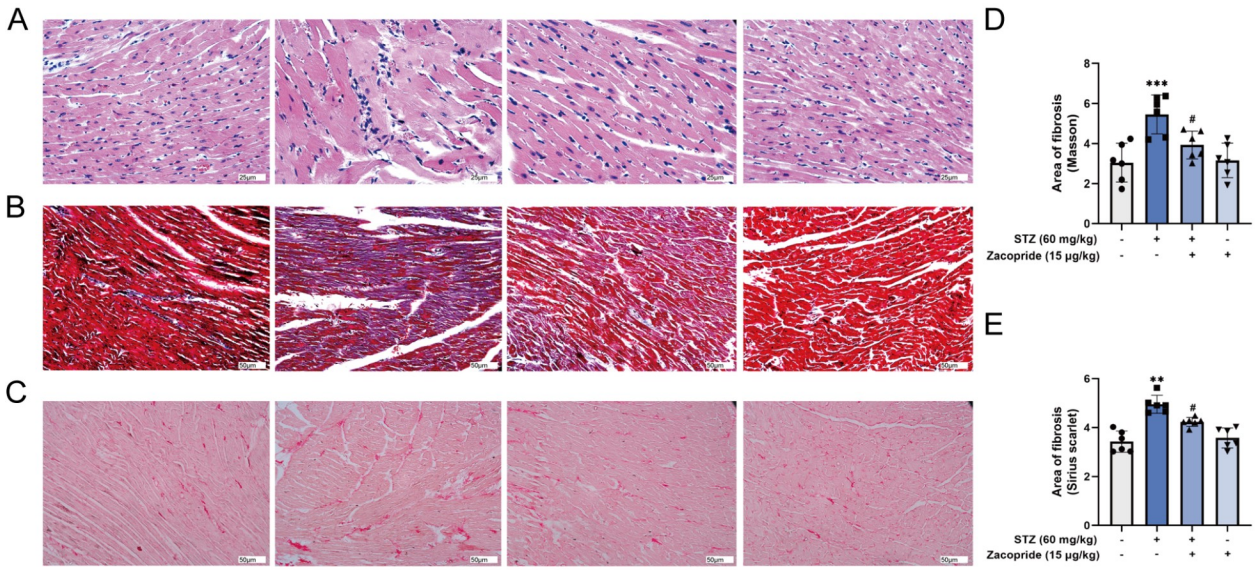

Figure 2. Zac improves myocardial tissue damage and fibrotic deposition (A) HE staining of left ventricular transverse sections (400 ×). (B) Masson trichrome staining showed the degree of left ventricular collagen deposition in rats (200 ×), red myocardial cells, and blue collagen fibres. (C) Sirius scarlet staining showed the deposition degree of collagen fibres in the left ventricle of rats (200 ×). The myocardial cells and collagen fibres were yellow and pink, respectively. (D,E) The statistical results of Masson trichrome staining and Sirius scarlet staining are expressed as the percentage of the total area of each region ($n = 6$). Data are presented as the mean ± SD. $^{**}P < 0.01$, $^{***}P < 0.001$ vs control; $^{\#}P < 0.05$ vs DCM.

proved that the expression of Kir2.1 protein was downregulated, and the expressions of fibrosis-related proteins in the hearts of DCM rats were upregulated. Furthermore, Zac treatment inhibited the expressions of DCM-induced fibrosis-related proteins (Figure 3C). Meanwhile, both western blot analysis and immunohistochemical results were statistically significant (Figure 3B,D). The above results suggest that activation of Kir2.1 could improve myocardial fibrosis in diabetic cardiomyopathy rats.

High glucose induces fibrosis in cardiac fibroblasts with downregulation of Kir2.1 protein expression

Primary cardiac fibroblasts were extracted and treated with high glucose at a concentration of 25 mM for 24 h. Compared with those in the normal group, the expression levels of α-SMA, collagen I, and collagen III in the HG group were significantly increased, while the expression of the Kir2.1 protein was decreased (Figure 4A). Meanwhile, the results were statistically significant (Figure 4B). In contrast, the patch-clamp results showed that both the inward and outward currents of Kir2.1 were inhibited, and the current amplitude was reduced (Figure 4C) in the high glucose-induced myocardial fibrosis model. Immunofluorescence staining showed that this was consistent with western blot analysis results (Figure 4D–G). The above results indicated that high glucose increased the expressions of fibrosis-related proteins in cardiac fibroblasts and decreased the expression and function of the Kir2.1 protein.

Activation of Kir2.1 inhibits high glucose-induced cardiac fibroblast fibrosis

To further explore the effect of Kir2.1 activation on high glucose-induced cardiac fibroblast fibrosis, we pretreated neonatal rat primary cardiac fibroblasts with Zac for 30 min and then treated them with high glucose for 24 h. The results showed that compared with those in the HG group, the expression of Kir2.1 protein in the HG + Zac group was increased, and the expressions of the fibrosis-related proteins α-SMA, collagen I, and collagen III were decreased (Figure 5A). The results were statistically significant, while there was no significant difference between the Zac and normal groups (Figure 5B). Immunofluorescence assays showed that the expressions of fibrosis-related proteins decreased after Zac treatment (Figure 5C–F). The above results show that activation of Kir2.1 at

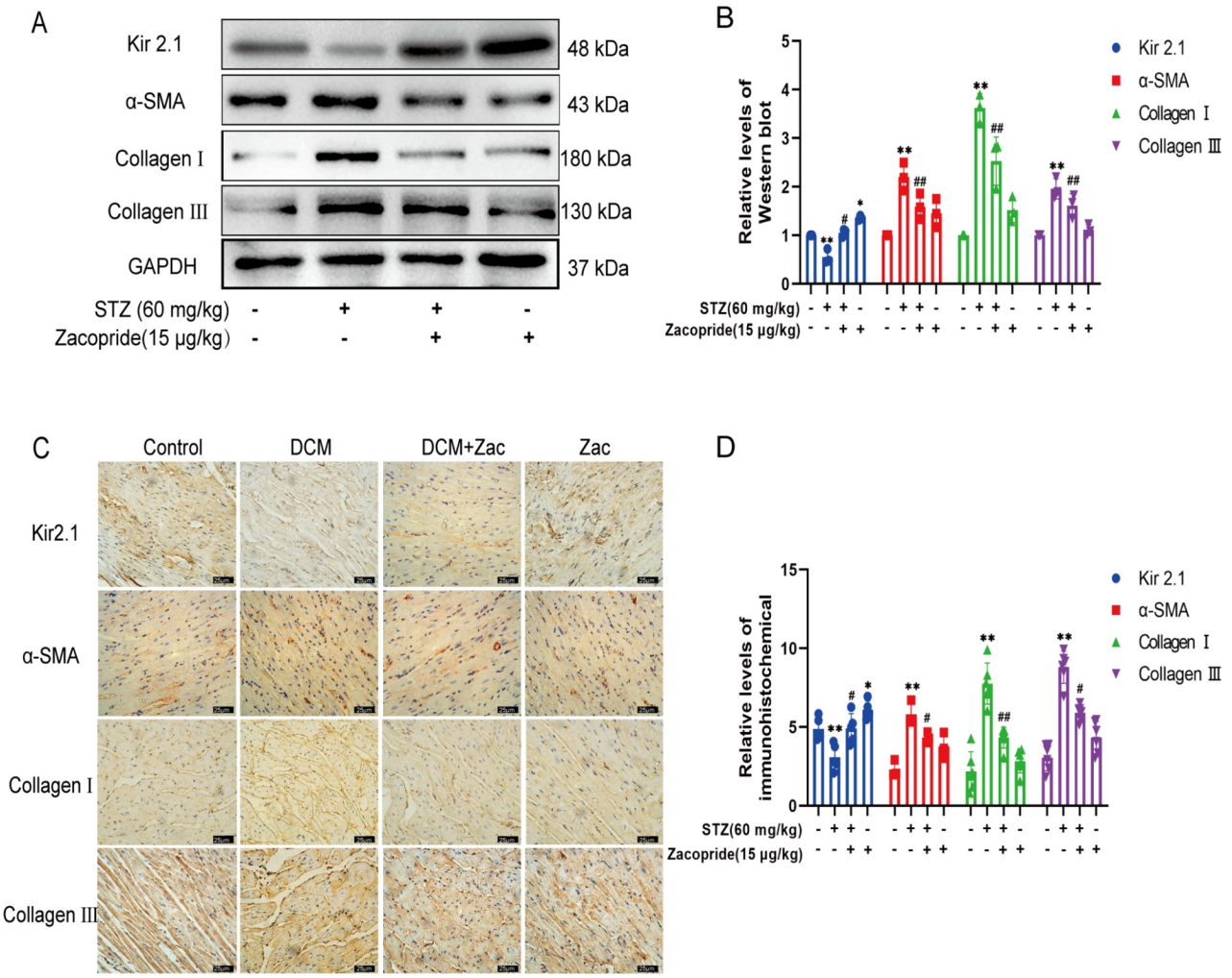

Figure 3. Zac upregulates the expression of myocardial Kir2.1 protein in DCM-induced rats and downregulates the expression of myocardial fibrosis proteins (A) Expressions of Kir2.1 protein and fibrosis-related proteins detected by western blot analysis ($n=3$). (B) Quantitative analysis of the changes in the expression levels of Kir2.1 and fibrosis-related proteins. (C) Immunohistochemical detection of Kir2.1 protein and fibrosis-related protein expressions (400 ×) ($n=6$). (D) Statistical analysis of Kir2.1, α-SMA, collagen I, and collagen III expression changes. All data were normalized to the control. Data are presented as the mean ± SD. $^{*}P<0.05$, $^{**}P<0.01$ vs control; $^{\#}P<0.05$, $^{\#\#}P<0.01$ vs DCM.

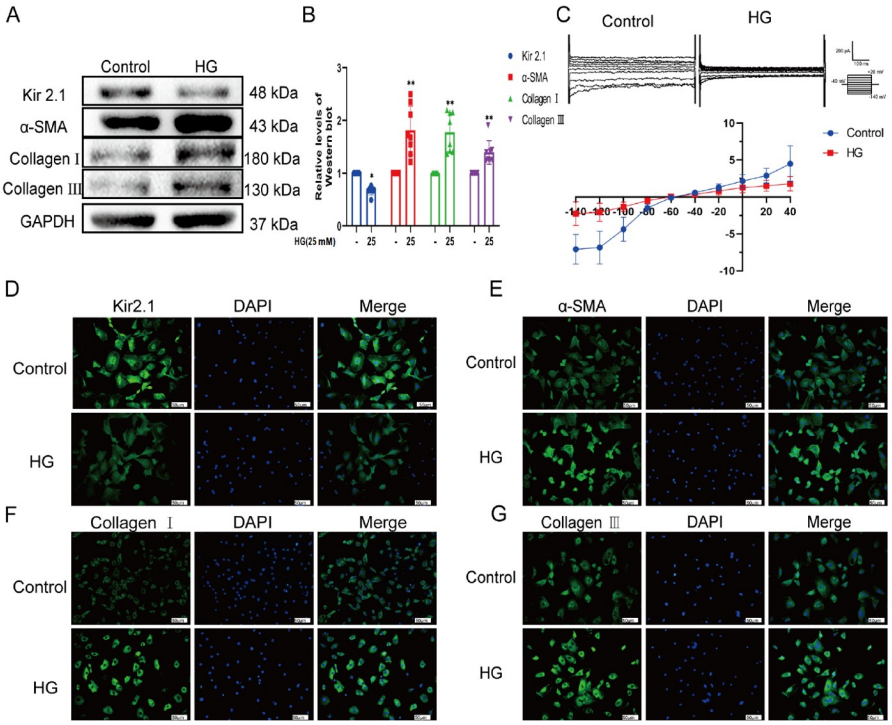

Figure 4. Cell-level verification of high glucose-induced cardiac fibroblast fibrosis-related protein changes and Kir2.1 protein and functional changes (A) Protein expression levels of Kir2.1, α-SMA, collagen I, and collagen III detected by western blot analysis ($n=8$). (B) Quantitative analysis of Kir2.1, α-SMA, collagen I, and collagen III protein expressions. (C) The Kir2.1 membrane current and I–V curves. (D–G) Semi-quantitative analysis of Kir2.1, α-SMA, collagen I, and collagen III fluorescence intensity (200 ×) ($n=3$). Data are shown as the mean ± SD. $^{*}P<0.05$, $^{**}P<0.01$ vs control.

the cellular level could inhibit high glucose-induced myocardial fibrosis.

Activation of Kir2.1 inhibits high glucose-induced calcium overload in cardiac fibroblasts and reduces the expressions of TGF-β1/Smad signaling pathway proteins

To explore how activation of Kir2.1 inhibits high glucose-induced cardiac fibroblast fibrosis, we used calcium probes to detect changes in intracellular calcium concentration and performed western blot analysis to detect changes in TGF-β1/Smad signaling pathway protein expression. As shown in Figure 6A,C, compared with the normal group, the intracellular free calcium concentration of cardiac fibroblasts induced by high glucose was significantly increased, and Zac treatment reduced HG-induced calcium overload. Western blot analysis results showed that compared with those in the normal group, the protein expression levels of TGF-β1 and p-Smad 2/3 in the HG group were increased significantly, and the protein expression levels of TGF-β1 and p-Smad 2/3 were decreased after Zac treatment. The expression levels of TGF-β1 and p-Smad 2/3 in the Zac group were not significantly different from those in the normal group (Figure 6B,D–F). The above results suggest that activation of Kir2.1 may inhibit cardiac fibroblast fibrosis by reducing calcium overload and the TGF-β1/Smad signaling pathway.

Discussion

In recent years, the incidence of diabetes in younger people has been increasing, and DCM is the leading cause of diabetes-related death [10,11]. Although the clinical treatment of myocardial fibrosis in DCM has been carried out, the results are still unsatisfactory [12,13]. Therefore, it is urgent to explore the pathogenesis of diabetic cardiomyopathy to find new targets and therapeutic methods.

The cardiac structural changes caused by DCM are as follows: myocardial hypertrophy leads to increased left ventricular weight, collagen deposition, and interstitial fibrosis, and ultimately, the heart hardens and is remodelled. In terms of function, DCM is characterized by an initial decline in diastolic function. As the disease progresses to intermediate and late stages, systolic function is also affected accordingly [14,15]. In this study, the diabetic cardiomyopathy model was prepared by intraperitoneal injection of STZ. After 12 weeks of modelling, we found that LVIDd and LVIDs of the ventricular wall structure were increased, and LVEF and LVFS of systolic cardiac function were significantly decreased, indicating abnormal cardiac function and successful modelling. These results were consistent with the modelling reported previously [16,17]. In addition, immunohistochemical staining showed that the myocardial fibres of the rats in the model group were damaged and broken, and many small necrotic foci were visible. Moreover, the cell collagen levels were increased, the arrangement was disorganized, and the expression levels of fibrosis-related proteins were increased, suggesting that DCM rats experienced severe pathological fibrosis. It has been reported that high glucose induces apoptosis, autophagy, proliferation, migration, and fibrosis of fibroblasts [18,19]. High glucose can also promote the transdifferentiation of myofibroblasts and activate the transcription and secretion of extracellular matrix proteins by regulating the production of reactive oxygen species and signal transduction *in vitro*. In

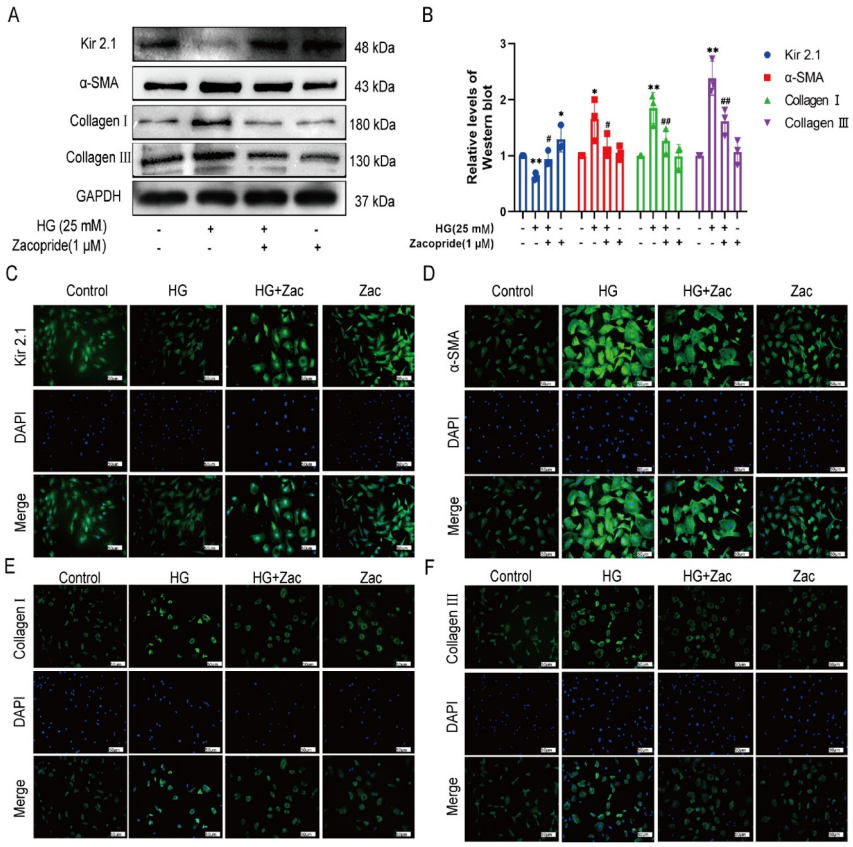

Figure 5. Activation of Kir2.1 inhibits high glucose-induced fibrosis-related protein expressions (A) Protein expression levels of Kir2.1, α-SMA, collagen I, and collagen III detected by western blot analysis. (B) The protein expression levels of Kir2.1, α-SMA, collagen I, and collagen III were quantitatively analyzed. (C–F) Semi-quantitative analysis of Kir2.1, α-SMA, collagen I, and collagen III fluorescence intensity (200 ×) ($n = 3$). Data are presented as the mean ± SD. $^{*}P < 0.05$, $^{**}P < 0.01$ vs control; $^{\#}P < 0.05$, $^{\#\#}P < 0.01$ vs HG.

this study, cardiac fibroblasts were induced by high glucose. The results showed that the expressions of α-SMA, collagen I, collagen III, and other fibrosis-related proteins were increased, suggesting that the *in vitro* high glucose-induced fibrosis model was successful.

The inwards potassium ion channel plays an essential physiological role in maintaining the stability of the cell resting membrane potential and excitable cells [20]. It has been reported that the upregulation of IK1 in atrial muscle may affect atrial electrophysiological activity. Qi *et al.* [21] found that in a heart failure model induced by rapid pacing in dogs, the functional expression of the Kir2.1 channel in atrial fibroblasts was upregulated, which promoted the proliferation of fibroblasts and thus formed the structural basis for atrial remodelling and atrial fibrillation. These results showed that IK1 in atrial fibroblasts and atrial myocyte had similar electrophysiological changes in heart failure. Interestingly, Liu *et al.* [22] found that there are molecular mechanisms for different effects of IK1 in the rat ventricular and atrial myocardium; the downregulation of IK1 is an important feature of ventricular EMG remodelling in heart failure [21]. Zhang *et al.* [23] also reported that hyperoside reduced the arrhythmia caused by myocardial ischemia-reperfusion by upregulating the expression of Kir2.1 protein and thus playing a protective role in the ventricular myocardium. In this study, we found that the expression of Kir2.1 protein and its fluorescence were reduced in cardiac fibroblasts treated with high glucose. Additionally, the current amplitude of Kir2.1 in the high glucose group was weaker than that in the normal group. The above results suggested that Kir2.1 protein and function were downregulated after high glucose intervention. We selected the Kir2.1 selective agonist Zac to explore its specific mechanism, which showed an exciting effect on rat ventricular myocytes, IK1, for pretreatment [9]. Liu *et al.* [8] found that Zac significantly improved myocardial infarction and isoproterenol-induced ventricular remodelling, but it had no significant effect on atrial IK1. In this study, Zac pretreatment was used in the DCM model. The results showed that Zac treatment significantly improved cardiac function and reduced collagen fibre deposition in DCM rats. *In vitro* and *in vivo* demonstration of the downregulation of fibrosis-related protein expression by Zac administration suggests a protective effect of Kir2.1 activation on high glucose-induced fibrosis, and the specific mechanisms need to be further explored.

Fauconnier *et al.* [24] confirmed that the elevated intracellular Ca^{2+} concentration of ventricular myocytes in heart failure rats could inhibit IK1. However, some studies have noted that Zac itself does not cause significant changes in voltage-gated Ca^{2+} current but reduces calcium overload by activating IK1, thereby inhibiting the signal transduction pathway of Ca^{2+} activation [25]. This also suggests that there is a certain relationship between IK1 and Ca^{2+}. Kir2.1, as a subtype playing an important role in IK1, may also play an important role. Li *et al.* [26] found that calcium chelators ameliorated TGF-β1-induced fibrosis in cardiac fibroblasts. Additionally, in a high glucose-induced diabetic cardiomyopathy model, calcium-sensitive receptor expression was upregulated in cardiac

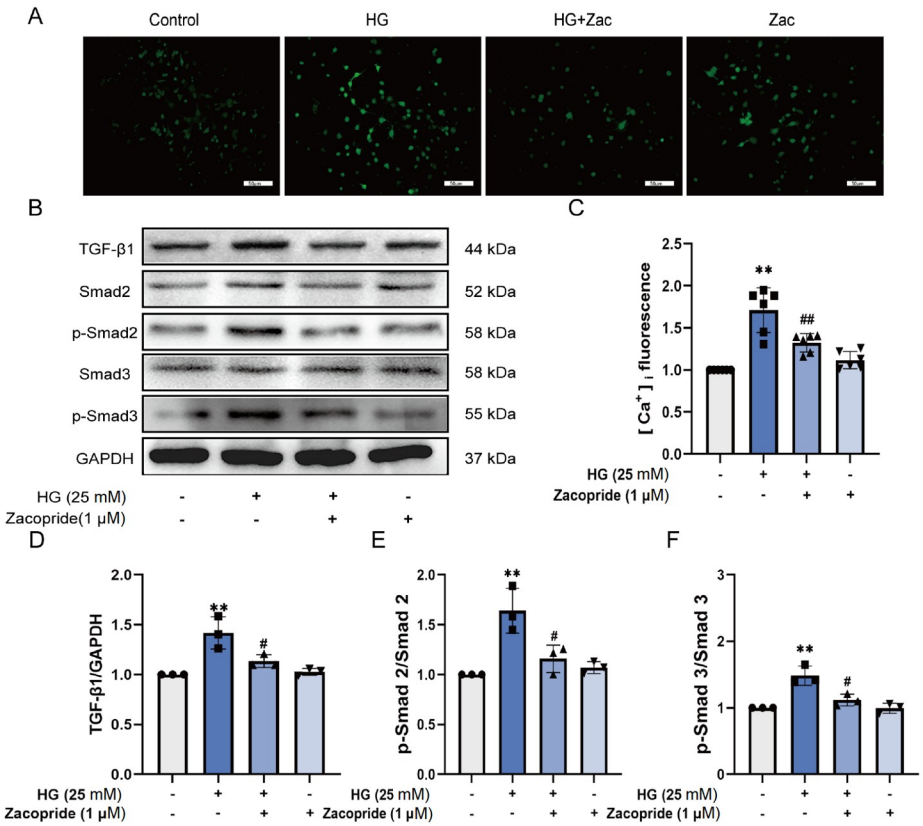

Figure 6. Zac inhibits calcium overload in CFs induced by high glucose and reduces the expressions of TGF-β1/Smad pathway proteins (A) Fluorescence image of cardiac fibroblasts induced by HG loaded with Fluo-3/AM (200×) ($n=6$). (B) Protein expression levels of TGF-β1, p-Smad2/Smad2, and p-Smad3/Smad3 detected by western blot analysis ($n=3$). (C) Quantitative analysis of the intracellular calcium concentration in each group. (D–F) Quantitative analysis of TGF-β1, p-Smad2/Smad2, and p-Smad3/Smad3 protein expressions. Data are presented as the mean ± SD. $^{**}P<0.01$ vs control; $^{\#}P<0.05$, $^{\#\#}P<0.01$ vs HG.

fibroblasts, leading to an increase in intracellular Ca^{2+} [3,27], which further activated the TGF-β1/Smad pathway and ultimately led to myocardial fibrosis. This suggests an interrelation between the calcium and TGF-β signaling pathways. In addition, in arrhythmia models, the nonspecific activator of PKC, PMA, also leads to a 41% reduction in the IK1 current, and mutations in the PKC phosphorylation site inhibit the effect of PMA [28]. Further mutation of the PKA phosphorylation site S425 to Leucine completely eliminates the agonistic effect of Zac on Kir2.1, thus suggesting that Zac selectively activates Kir2.1 channels through the PKA-mediated signaling pathway [29]. We further explored the specific protective mechanism of Kir2.1 activation on high glucose-induced myocardial fibrosis at the cellular level. We found that Zac reduced the intracellular Ca^{2+} concentration and inhibited the protein expressions of TGF-β1, p-Smad2, and p-Smad3 in fibrosis-related signaling pathways. Therefore, we hypothesize that activation of Kir2.1 may inhibit cardiac fibroblast fibrosis and ameliorate the development of DCM by reducing the intracellular Ca^{2+} concentration and the TGF-β1/Smad signaling pathway.

In summary, this study demonstrates that activation of Kir2.1 protects the heart from DCM-induced myocardial fibrosis, which is mediated by Ca^{2+} and the TGF-β1/Smad signaling pathway (Figure 7). Nevertheless, there are limitations in our study. The interrelationship between calcium flux and the TGF-β1/Smad signaling pathway as well as other mechanisms by which Kir2.1 is involved in regulating STZ-induced myocardial fibrosis will be further refined in our future studies. We will also continue to explore the pathogenesis of diabetic cardiomyopathy, new targets and therapeutic approaches.

Activation of Kir2.1 may improve diabetic cardiomyopathy-induced fibrosis by inhibiting Ca^{2+} and the TGF-β1/Smad signaling pathways, which may provide a new theoretical basis for the clinical treatment of the disease.

Funding

This work was supported by the grants from the National Natural Science Foundation of China (Nos. 81860286 and 81660271), the Corps Science and Technology Cooperation Project of China (No. 2020BC004), the Nonprofit Central Research Institute Fund of Chinese Academy of Medical Sciences (No. 2020-PT330-003), the Youth Innovation Talent Cultivation Project of Shihezi University (No. CXPY202215), the Self-funded Project of Shihezi University (No. ZZZC202140), and the Scientific Research Project of Shihezi University (No. ZZZC201954A).

References

1. Zhang W, Xu W, Feng Y, Zhou X. Non-coding RNA involvement in the pathogenesis of diabetic cardiomyopathy. *J Cell Mol Med* 2019, 23: 5859–5867
2. Ma ZG, Yuan YP, Wu HM, Zhang X, Tang QZ. Cardiac fibrosis: new insights into the pathogenesis. *Int J Biol Sci* 2018, 14: 1645–1657
3. Yuan H, Fan Y, Wang Y, Gao T, Shao Y, Zhao B, Li H, *et al.*

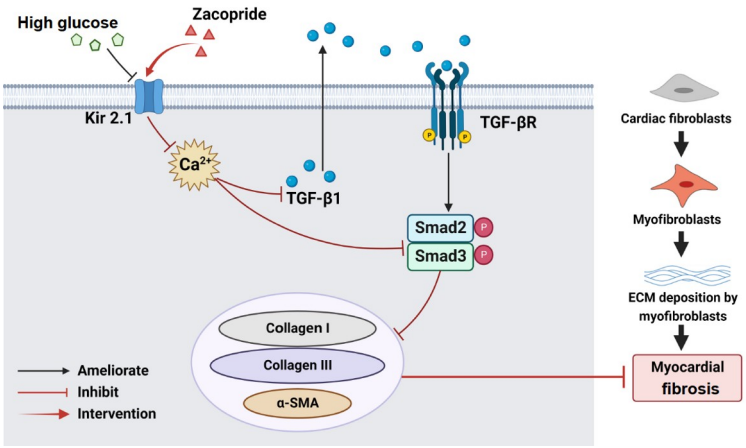

Figure 7. Kir2.1 regulates the Ca^{2+} and TGF-β1/Smad signaling pathways and participates in the process of high glucose-induced cardiac fibroblast fibrosis

Calcium-sensing receptor promotes high glucose-induced myocardial fibrosis via upregulation of the TGF-β1/Smads pathway in cardiac fibroblasts. *Mol Med Report* 2019, 20: 1093–1102

4. Lindner D, Zietsch C, Tank J, Sossalla S, Fluschnik N, Hinrichs S, Maier L, *et al.* Cardiac fibroblasts support cardiac inflammation in heart failure. *Basic Res Cardiol* 2014, 109: 428
5. Stewart L, Turner NA. Channelling the force to reprogram the matrix: mechanosensitive ion channels in cardiac fibroblasts. *Cells* 2021, 10: 990
6. Grandi E, Sanguinetti MC, Bartos DC, Bers DM, Chen-Izu Y, Chiamvimonvat N, Colecraft HM, *et al.* Potassium channels in the heart: structure, function and regulation. *J Physiol* 2017, 595: 2209–2228
7. van Vliet P, de Boer TP, van der Heyden MAG, El Tamer MK, Sluijter JPG, Doevendans PA, Goumans MJ. Hyperpolarization induces differentiation in human cardiomyocyte progenitor cells. *Stem Cell Rev Rep* 2010, 6: 178–185
8. Liu QH, Qiao X, Zhang LJ, Wang J, Zhang L, Zhai XW, Ren XZ, *et al.* IK1 channel agonist zacopride alleviates cardiac hypertrophy and failure via alterations in calcium dyshomeostasis and electrical remodeling in rats. *Front Pharmacol* 2019, 10: 929
9. Liu QH, Li XL, Xu YW, Lin YY, Cao JM, Wu BW. A novel discovery of IK1 channel agonist. *J Cardiovasc Pharmacol* 2012, 59: 37–48
10. Dei Cas A, Fonarow GC, Gheorghiade M, Butler J. Concomitant diabetes mellitus and heart failure. *Curr Problems Cardiol* 2015, 40: 7–43
11. Jia G, Whaley-Connell A, Sowers JR. Diabetic cardiomyopathy: a hyperglycaemia- and insulin-resistance-induced heart disease. *Diabetologia* 2018, 61: 21–28
12. Bacmeister L, Schwarzl M, Warnke S, Stoffers B, Blankenberg S, Westermann D, Lindner D. Inflammation and fibrosis in murine models of heart failure. *Basic Res Cardiol* 2019, 114: 19
13. Ahmed U, Khaliq S, Ahmad HU, Ahmad I, Ashfaq UA, Qasim M, Masoud MS. Pathogenesis of diabetic cardiomyopathy and role of miRNA. *Crit Rev Eukaryot Gene Expr* 2021, 31: 79–92
14. Murtaza G, Virk HUH, Khalid M, Lavie CJ, Ventura H, Mukherjee D, Ramu V, *et al.* Diabetic cardiomyopathy—a comprehensive updated review. *Prog Cardiovasc Dis* 2019, 62: 315–326
15. Frangogiannis NG. Cardiac fibrosis. *Cardiovasc Res* 2021, 117: 1450–1488
16. Zhang J, Qiu H, Huang J, Ding S, Huang B, Wu Q, Jiang Q. Establishment of a diabetic myocardial hypertrophy model in Mus musculus castaneus mouse. *Int J Exp Path* 2018, 99: 295–303
17. Shepherd DL, Nichols CE, Croston TL, McLaughlin SL, Petrone AB, Lewis SE, Thapa D, *et al.* Early detection of cardiac dysfunction in the type 1 diabetic heart using speckle-tracking based strain imaging. *J Mol Cell Cardiol* 2016, 90: 74–83
18. Lim W, Park S, Bazer FW, Song G. Naringenin-induced apoptotic cell death in prostate cancer cells is mediated via the PI3K/AKT and MAPK signaling pathways. *J Cell Biochem* 2017, 118: 1118–1131
19. Gu X, Fang T, Kang P, Hu J, Yu Y, Li Z, Cheng X, *et al.* Effect of ALDH2 on high glucose-induced cardiac fibroblast oxidative stress, apoptosis, and fibrosis. *Oxid Med Cell Longev* 2017, 2017: 1–12
20. Liu C, Liu E, Luo T, Zhang W, He R. Opening of the inward rectifier potassium channel alleviates maladaptive tissue repair following myocardial infarction. *Acta Biochim Biophys Sin* 2016, 48: 687–695
21. Qi XY, Huang H, Ordog B, Luo X, Naud P, Sun Y, Wu CT, *et al.* Fibroblast inward-rectifier potassium current upregulation in profibrillatory atrial remodeling. *Circ Res* 2015, 116: 836–845
22. Liu QH, Zhang LJ, Wang J, Wu BW, Cao JM. Cardioprotection of an IK1 channel agonist on L-thyroxine induced rat ventricular remodeling. *Am J Transl Res* 2021, 13: 8683–8696
23. Zhang CY, Yang Q. Effects of hyperoside preconditioning on myocardial ATPase activity and expression of Cx43 and Kir2.1 in rats with myocardial ischemia reperfusion arrhythmia. *Chinese Patent Medicine* 2018, 40: 254–260
24. Fauconnier J, Lacampagne A, Rauzier J, Vassort G, Richard S. Ca-dependent reduction of I in rat ventricular cells: a novel paradigm for arrhythmia in heart failure? *Cardiovasc Res* 2005, 68: 204–212
25. Lu L, Guo J, Hua Y, Huang K, Magaye R, Cornell J, Kelly DJ, *et al.* Cardiac fibrosis in the ageing heart: contributors and mechanisms. *Clin Exp Pharmacol Physiol* 2017, 44: 55–63
26. Li W, Zhang Z, Li X, Cai J, Li D, Du J, Zhang B, *et al.* CGRP derived from cardiac fibroblasts is an endogenous suppressor of cardiac fibrosis. *Cardiovasc Res* 2020, 116: 1335–1348
27. Duran J, Troncoso M, Lagos D, Ramos S, Marin G, Estrada M. GDF11 modulates Ca^{2+}-dependent smad2/3 signaling to prevent cardiomyocyte hypertrophy. *Int J Mol Sci* 2018, 19: 1508
28. Karle CA, Zitron E, Zhang W, Wendt-Nordahl G, Kathöfer S, Thomas D, Gut B, *et al.* Human cardiac inwardly-rectifying K^+ channel $Kir_{2.1b}$ is inhibited by direct protein kinase C-dependent regulation in human isolated cardiomyocytes and in an expression system. *Circulation* 2002, 106: 1493–1499
29. Zhang L, Liu QH, Liu CF, Zhai XW, Feng QL, Xu RL, Cui XL, *et al.* Zacopride selectively activates the Kir2.1 channel via a PKA signaling pathway in rat cardiomyocytes. *Sci China Life Sci* 2013, 56: 788–796